Phototransduction in primate cones and blowfly photoreceptors

Hateren, J.H. van; Snippe, H.P.

Published in:
Journal of comparative physiology a-Neuroethology sensory neural and behavioral physiology

DOI:
10.1007/s00359-005-0060-y

Publication date:
2006

J Comp Physiol A (2006) 192: 187–197
DOI 10.1007/s00359-005-0060-y

ORIGINAL PAPER

J. H. van Hateren · H. P. Snippe

Phototransduction in primate cones and blowfly photoreceptors: different mechanisms, different algorithms, similar response

Received: 22 June 2005 / Revised: 14 September 2005 / Accepted: 18 September 2005 / Published online: 25 October 2005

Abstract Phototransduction in primate cones is compared with phototransduction in blowfly photoreceptor cells. Phototransduction in the two cell types utilizes not only different molecular mechanisms, but also different signal processing steps, producing range compression, contrast constancy, and an intensity-dependent integration time. The dominant processing step in the primate cone is a strongly compressive nonlinearity due to cGMP hydrolysis by phosphodiesterase. In the blowfly photoreceptor a considerable part of the range compression is performed by the nonlinear membrane of the cell. Despite these differences, both photoreceptor cell types are similarly effective in compressing the wide range of naturally occurring intensities, and in converting intensity variations into contrast variations. A direct comparison of the responses to a natural time series of intensities, simulated in the cone and measured in the blowfly photoreceptor, shows that the responses are quite similar.

Keywords Photoreceptors · Sensory transduction · Light adaptation · Dynamic range · Natural stimuli

Introduction

Light intensities in outdoor environments vary considerably. Several factors contribute to this variation: the sun's elevation varies during the day and during the year, lighting conditions vary across environments, the cloud cover varies, and there are variations produced by uneven illumination and differences in reflectance within scenes in a particular environment. In this article, we will consider the consequences of the latter source of intensity variations, which can cover a range of 10^4 and more in sunlit scenes (van Hateren 1997). The visual systems of animals navigating through a particular environment are therefore exposed to strongly and quickly varying intensities. Because the dynamic range of these intensity variations is larger than the range that can be encoded linearly by photoreceptor cells, these cells possess mechanisms of sensitivity regulation. A prominent mechanism regulating sensitivity is the process of phototransduction, transducing absorbed photons into currents and voltages across the cell's membrane.

Phototransduction has been extensively studied in the rods and cones of vertebrate eyes (see reviews of Pugh and Lamb 2000; Burns and Baylor 2001; Fain et al. 2001). Absorption of light leads to a reduction of a standing photocurrent, resulting in a hyperpolarization of the membrane potential. In contrast, phototransduction in most invertebrate eyes, well studied in several species (see reviews of Minke and Hardie 2000; Nasi et al. 2000; Hardie and Raghu 2001), leads to an increase of photocurrent in response to light absorption, and therefore a depolarization of the membrane potential. This difference between vertebrate and invertebrate phototransduction is due to differences in the molecular mechanisms involved.

In this article we will compare the two basic schemes of phototransduction under daylight conditions, as exemplified by the characteristics of primate cones and blowfly photoreceptors. We will review the differences between the key molecular mechanisms involved, and argue that also the processing tactics, i.e., the algorithms, are different. Nevertheless, it will become clear that the general strategy, as reflected in the overall input–output characteristics of the two types of photoreceptors, is remarkably similar for such clearly unrelated species. We will argue that this can be understood as an adaptation to the properties of natural stimuli. Firstly, the large dynamic range of such stimuli requires response compression. Secondly, contrast in a visual scene is independent of the level of illumination, which makes it attractive for photoreceptors to encode

J. H. van Hateren (✉) · H. P. Snippe
Department of Neurobiophysics, University of Groningen, Nijenborgh 4, NL-9747 AG Groningen, The Netherlands
E-mail: j.h.van.hateren@rug.nl
Tel.: +31-50-3634788
Fax: +31-50-3634740

contrast rather than light intensity. Finally, increased photon noise at reduced light levels is counteracted by both photoreceptor types by increasing the integration time at such levels.

Materials and methods

The cone responses as shown in Figs. 5b and 6b were simulated using a recently developed model of the primate cone (van Hateren 2005), using the generic model parameters defined there and assuming a mean illuminance of 300 td for the stimulus. The response of a three times faster cone (Figs. 5c, 6c) was computed with the same model and generic model parameters, but with all time constants in the model reduced by a factor of three.

Responses in blowfly (*Calliphora vicina*) photoreceptor cells (R1-6) were obtained using standard intracellular recording techniques, with natural time series presented through a bright light emitting diode (details on stimulus and measurement are provided in van Hateren 1997 and van Hateren and Snippe 2001). Figures 5d and 6d show the response to a single stimulus presentation of a single photoreceptor cell; similar responses were measured in seven photoreceptor cells. The mean stimulus intensity was at a daylight level estimated to be of the same order of magnitude as used for the cone simulation.

Results

Below we will first review the mechanism and processing stages of phototransduction in primate cones and blowfly photoreceptors, respectively, and subsequently show their responses to a natural time series of intensities.

Phototransduction in primate cones

Figure 1 (top row) shows the key processes of phototransduction in the primate cone, following van Hateren (2005). Light I is absorbed by visual pigment, R, in the outer segment of the cone. Activated pigment R^* is subsequently removed (skew arrow in the figure). The transition from I to R^* represents a low-pass filter, with a time constant inversely proportional to the removal rate of R^* (e.g., Pugh and Lamb 2000). R^* activates a G-protein, which then binds to phosphodiesterase, PDE, to form an active complex E^*. This second step, from R^* to E^*, also represents a low-pass filter. Because one R^* produces many E^*, the dominant functions of these first stages are amplification and low-pass filtering.

The next step is hydrolysis of cGMP by E^*. Non-activated PDE can also hydrolyze cGMP, although considerably less effectively than E^*, and therefore the hydrolysis of cGMP is governed by a rate

$$\beta = c_\beta + k_\beta E^*, \tag{1}$$

with c_β and k_β constants (Nikonov et al. 2000; van Hateren 2005). With cGMP being produced at a rate α, the change in cGMP concentration per unit of time is given by the difference in cGMP production and removal, thus

$$\frac{\mathrm{d}X}{\mathrm{d}t} = \alpha - \beta X, \tag{2}$$

with $X = [\mathrm{cGMP}]$. This is an important equation, forming the key to understanding the main strategy of phototransduction in cones. This equation can be considered as an input–output filter, with β as the input (because it is driven by the light intensity) and X as the output. It is a nonlinear equation, because the input β is multiplied by the output X. This nonlinearity has two consequences. Firstly, it produces a highly nonlinear relationship between β and X, effectively producing strong response compression. Secondly, it produces an effective integration time that decreases with increasing β, i.e., with increasing light levels (Nikonov et al. 2000; van Hateren 2005). The first effect, response compression, can be best understood by assuming for the moment that the cGMP production rate, α, is a constant (as it would be, e.g., under conditions of Ca^{2+} clamping). The steady-state of Eq. 2 is then given by $\mathrm{d}X/\mathrm{d}t = 0$, thus

$$0 = \alpha - \beta X, \quad \text{or } X = \alpha\frac{1}{\beta}. \tag{3}$$

This equation can be interpreted as follows: the original input β is first inverted to yield $1/\beta$, and subsequently $1/\beta$ is multiplied by a gain α to yield the output X.

The dynamic behavior of Eq. 2 can be understood in a similar way by rewriting it as

$$\tau_\beta \frac{\mathrm{d}X}{\mathrm{d}t} = \alpha\frac{1}{\beta} - X, \quad \text{with} \quad \tau_\beta = 1/\beta. \tag{4}$$

We can compare this equation with the standard equation describing low-pass filtering an input x into an output y (e.g., van Hateren 2005) with unity gain and a time constant τ:

$$\frac{\mathrm{d}y}{\mathrm{d}t} + y/\tau = x/\tau, \quad \text{or} \quad \tau\frac{\mathrm{d}y}{\mathrm{d}t} = x - y. \tag{5}$$

It is then clear that Eq. 4 can be interpreted as a sequence of the following processes: the signal β is first transformed into a signal $1/\beta$, then $1/\beta$ is multiplied by a gain α, and the result is finally low-pass filtered with a time constant τ_β to yield X. Note that Eq. 4 is still highly nonlinear, firstly because of the $1/\beta$ operation, and secondly because the time constant $\tau_\beta = 1/\beta$ is not really a constant, but an adaptive parameter, because β is a function of the input light level.

To conclude, the hydrolysis of cGMP by E^* has several functions. In addition to providing further amplification, because one E^* hydrolyzes many cGMP, its

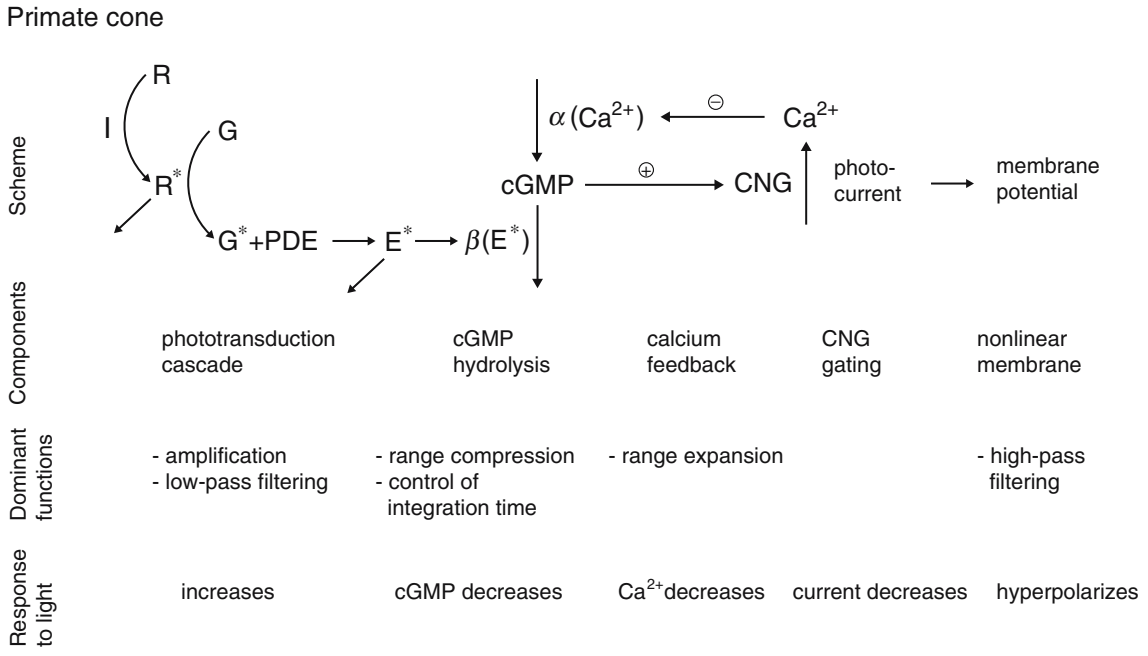

Fig. 1 Scheme of phototransduction in primate cones. Light, I, activates visual pigment, R. Activated R^* activates a G-protein, with G^* subsequently binding to PDE. PDE and E^* hydrolyze cGMP at a rate β. An increase in light intensity therefore reduces [cGMP], resulting in a closure of cyclic nucleotide-gated (CNG) channels, a reduction of photocurrent, a reduction of $[Ca^{2+}]$ in the cell, leading to a reduced production rate α of cGMP, thus completing the negative feedback loop on [cGMP]. The photocurrent finally produces, via a nonlinear membrane, the membrane potential of the cell. See the text for further discussion

two dominant functions are range compression, through $1/\beta$, and control of integration time, through $\tau_\beta = 1/\beta$.

Using $1/\beta$ for range compression is highly effective, in fact too effective. Figure 2a illustrates this. The light and dark gray segments on the intensity axis show two intensity ranges at tenfold different light levels, but of equal contrast: in both cases the range is mean intensity minus 25% until mean intensity plus 25%. In a natural scene, this could correspond to the contrast range on the surface of two identical objects viewed under tenfold different illumination levels, for example one in direct sunlight and the other in the shadow. A visual system that strives to take advantage of this invariant object property, i.e., constant contrast independent of illumination level, needs to convert the strongly different absolute intensity ranges of Fig. 2a into equally sized response ranges. Figure 2a shows that a $1/\beta$ nonlinearity overshoots this goal; after the transformation the response ranges are again strongly different, but now with the roles of the low and high light levels swapped. In other words, the $1/\beta$ nonlinearity is too compressive for reaching contrast constancy (see van Hateren 2005 for a formal derivation of this result).

The $1/\beta$ nonlinearity is also too strong for proper range compression. This is illustrated by the probability density functions (pdf) in the column on the right of Fig. 2. Figure 2d shows a theoretical pdf for the distribution of light intensities in natural environments (see Appendix). This pdf is quite skewed, with a long tail extending to much higher intensity values than shown in the graph. Figure 2e shows the pdf resulting from the $1/\beta$ transformation. The tail containing high intensities in Fig. 2d is now mapped to the peak at low values of $1/\beta$ in Fig. 2e, and vice versa. The pdf in Fig. 2e is only slightly less skewed than the pdf in Fig. 2d because of c_β (Eq. 1), which limits the maximum value $1/\beta$ can reach for $E^* \approx 0$, i.e., for low light intensities.

The too compressive nature of $1/\beta$ is corrected by the action of the calcium feedback loop (top row of Fig. 1), regulating α. This loop operates as follows (for quantitative details see van Hateren 2005). An increase in [cGMP], as occurs when the light level is reduced, opens more cyclic nucleotide-gated (CNG) channels in the outer segment. This increases the photocurrent entering the outer segment. Part of this photocurrent consists of Ca^{2+} ions, resulting in a rising Ca^{2+} concentration. This will then progressively inhibit the activity of guanylate cyclase, the enzyme responsible for the production of cGMP. Therefore, the initial increase of [cGMP] ultimately results in a decrease of the production of cGMP, which implies that the loop is in fact a negative feedback loop.

The calcium feedback loop can be shown to have two major effects. Firstly, it relaxes the nonlinear compression due to cGMP hydrolysis, by effectively expanding the dynamic range (Nikonov et al. 2000; van Hateren 2005). Secondly, it reduces the effect of $\tau_\beta = 1/\beta$ by increasing the frequency bandwidth of the system, in particular at low light levels (see the small-signal analysis in van Hateren 2005). The effect of the loop on contrast constancy and on the dynamic range is illustrated in Fig. 2, where we used the result that the photocurrent,

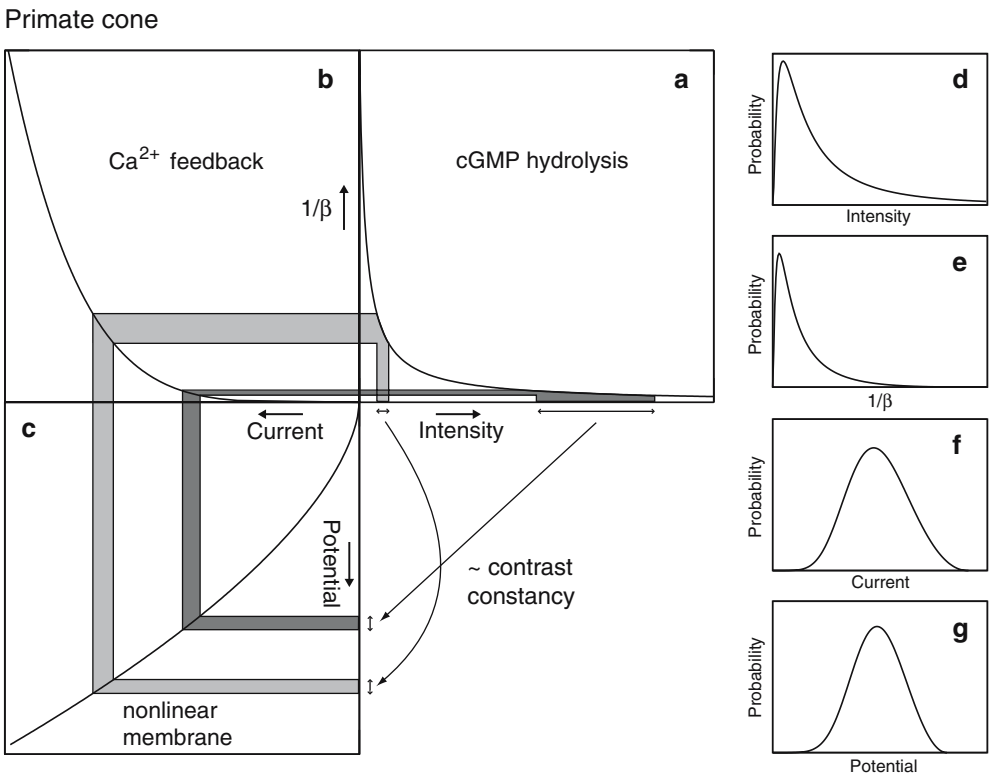

Fig. 2 Contrast constancy and range compression in primate cones. Identical contrasts at different light intensities I (*gray sections* at the intensity axis of **a**) transform, under steady-state conditions, as $1/\beta \sim 1/(\text{constant} + I)$ due to cGMP hydrolysis by PDE and E^*. The calcium feedback loop transforms this approximately as $(1/\beta)^{0.2}$ into photocurrent (**b**). The nonlinear membrane of the cell finally transforms the photocurrent I_p as $I_p^{0.6}$ into the membrane potential of the cell (**c**). **d**–**g** The probability density of natural intensities (**d**, see Appendix) is gradually transformed by the nonlinearities of (**a**–**c**)

I_p, is approximately proportional to $(1/\beta)^{0.2}$ as a result of the calcium feedback (van Hateren 2005). This follows from the fact that α is strongly inhibited by $[Ca^{2+}]$, approximately as $1/[Ca^{2+}]^4$. Using $[Ca^{2+}] \sim I_p$, we can therefore write for the steady-state of the feedback loop $I_p \sim (1/\beta)/I_p^4$, or $I_p \sim (1/\beta)^{0.2}$. Figure 2b shows that the range of photocurrent is now almost equal for equal contrast ranges at different light levels. Also the overly compressed dynamic range of Fig. 2e is converted to the more even distribution of photocurrents shown in Fig. 2f. Because the calcium feedback loop in effect expands the range occupied by high intensities, reversing the too strong compression by the $1/\beta$-nonlinearity, its main function is range expansion rather than range compression (see third row of Fig. 1).

The photocurrent I_p generated in the outer segment finally drives the nonlinear membrane of the inner segment to produce a membrane potential V_p, here defined relative to the membrane potential at zero photocurrent. The steady-state behavior of this processing stage can be described as V_p being proportional to $I_p^{0.6}$ (for quantitative details see van Hateren 2005). The corresponding curve (Fig. 2c) shows that the membrane contributes only slightly to contrast constancy. Also the effect on the pdf of the membrane voltage (Fig. 2g) as compared to the pdf of the photocurrent (Fig. 2f) is limited. Because the nonlinear properties of the membrane of the inner segment presumably have slow dynamics (van Hateren 2005), its dominant function appears to be a mild high-pass filtering (cf. for rods; Delmontis and Cervetto 2002; van Hateren 2005).

It should be noted that Fig. 2 presents the nonlinear transformations belonging to the steady state, i.e., it only provides a good approximation for fluctuations in the stimulus slower than the integration time of the cone. Nevertheless, a simulation of the dynamical response to long stretches of measured natural time series of intensities, like the one in Fig. 5, produces pdf's similar to those shown in Fig. 2. The main reason for this is that natural time series of intensities have a power spectrum dominated by low temporal frequencies (van Hateren 1997), and the steady-state characteristics of the cone therefore dominate the shape of the pdf's.

It should also be noted that the model for the cone used here does not include pigment bleaching, and therefore only applies to sub-bleaching light levels. When bleaching becomes strong, the cone response is expected to fully follow Weber's law (equal response to equal stimulus contrast), and the DC-level of the cone response is expected to remain fixed, independent of the light level. These effects will both contribute to range compression, and are in line with the conclusions of the present study.

Phototransduction in blowfly photoreceptors

Phototransduction in fly photoreceptors is not as well understood as it is in rods and cones. The nature of the second messenger driving the membrane channels has not yet been fully established, and there is also uncertainty about the mechanisms of gain control. It is known that

Ca^{2+} plays a crucial role in regulating the sensitivity and integration time of the photoreceptor (Hardie and Raghu 2001), but it is not fully known which processes in the transduction chain are targetted by Ca^{2+}, nor what their stochiometry is. We will therefore make several simplifying assumptions and hypotheses for the basic scheme presented below. First, we will restrict the discussion to bright, daylight intensities. At low light levels, a blowfly photoreceptor is essentially linear, because each of its microvilli is believed to act as an independent photon detector. However, this independence is lost at high light levels, presumably by coupling through the Ca^{2+} concentration in the cell body, producing a reduced gain of each microvillus. As a result, there is a nonlinear (compressive) relationship between light intensity and Ca^{2+} concentration (Oberwinkler and Stavenga 1998). We will assume below that the Ca^{2+} coupling of microvilli through the cell body is the dominating factor controlling sensitivity at high light levels. We therefore ignore several other known effects of Ca^{2+}, e.g., a Ca^{2+}-dependent positive feedback in the amplification stage (Hendersen et al 2000), which may be primarily important for ensuring large photon responses at low to intermediate light levels. Because the scheme does not aim at providing a detailed explanation of the dynamics of the response, we will also ignore the effect of latency variations on the response dynamics (Juusola and Hardie 2001).

Figure 3 shows the basic scheme, where we assume that the main processes in the phototranduction cascade in the blowfly are similar to those in the fruitfly *Drosophila*, which has been more extensively investigated (Montell 1999; Hardie and Raghu 2001). Light I is absorbed by visual pigment R, and the activated pigment R^* subsequently activates a G-protein. G^* then activates phospholipase C (PLC), which produces diacylglycerol (DAG) from PIP_2 (phosphatidylinositol 4,5-biphosphate). There is good evidence that DAG (or possibly one of its metabolites) is the second messenger responsible for opening the membrane channels (TRP) generating the photocurrent (Hardie 2003). With DAG being produced at a rate β, and removed (or inactivated) at a rate α, the change in DAG concentration per unit of time is given by the difference in DAG production and removal, thus

$$\frac{dX}{dt} = \beta - \alpha X, \tag{6}$$

with $X = [\text{DAG}]$. This equation can be considered as an input–output filter, with β as the input (because it is driven by the light intensity) and X as the output. Assuming for the moment that α is a constant, Eq. 6 is just a linear equation (a first-order low-pass filter) relating the input β to the output X. The equation is therefore quite different from the corresponding Eq. 2 for the primate cone, which represents not a linear, but a highly nonlinear filter. The role of α becomes clear when rewriting the equation as

$$\tau_\alpha \frac{dX}{dt} = \frac{1}{\alpha}\beta - X, \quad \text{with} \quad \tau_\alpha = 1/\alpha. \tag{7}$$

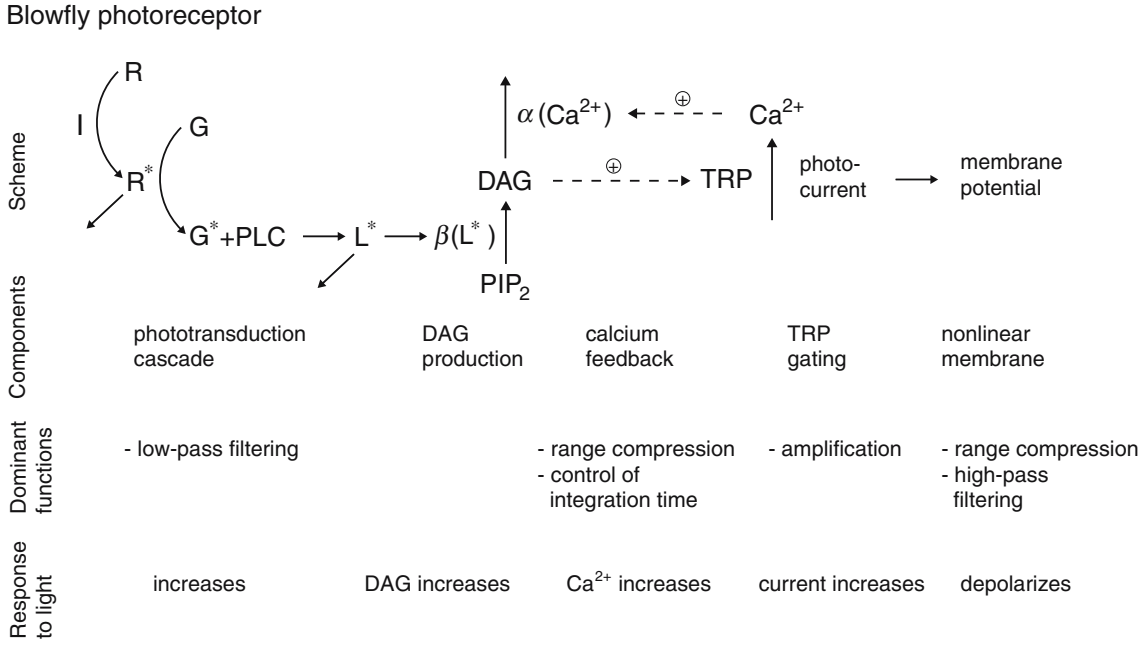

Fig. 3 Scheme of phototransduction in blowfly photoreceptor cells. Light, I, activates visual pigment, R. Activated R^* activates a G-protein, with G^* subsequently binding to PLC. Activated PLC, L^*, produces DAG at a rate β. An increase in light intensity therefore increases [DAG], resulting in an opening of TRP channels, an increase of photocurrent, an increase of $[Ca^{2+}]$ in the cell, presumably leading to an increased inactivation rate α of DAG, thus completing the negative feedback loop on [DAG]. The photocurrent finally produces, via a nonlinear membrane, the membrane potential of the cell. See the text for further discussion

Comparing this with the standard equation for a unity gain low-pass filter, Eq. 5, we see that Eq. 7 can be interpreted as a sequence of linear processes: the input signal β is first multiplied by a gain $1/\alpha$, and subsequently low-pass filtered with a time constant τ_α to yield X.

In reality, the photoreceptor is not linear as suggested by Eq. 7, but reduces its gain with inceasing light intensity, presumably regulated by the Ca^{2+} concentration in the cell. Although the nature and stochiometry of the interactions of Ca^{2+} with the transduction chain are not fully known, the steady-state Ca^{2+} concentration has been measured by fluorometry as a function of light intensity (Oberwinkler and Stavenga 1998). On a double-logarithmic scale, $[Ca^{2+}]$ is linearly related to the light intensity over a considerable intensity range, with a slope of approximately 0.5 (Fig. 6c of Oberwinkler and Stavenga 1998). If we assume that β is directly proportional to the light intensity, and that the photocurrent I_p is directly proportional to $[Ca^{2+}]$, this implies that I_p is proportional to $\beta^{0.5}$. In other words, there is a compressive (square-root) relationship between light intensity and photocurrent. The simplest way to explain this square-root behavior is shown in Fig. 3 by the dashed lines (indicating that this loop is hypothetical, and may be more complex than depicted here). It produces both a decrease in sensitivity and a decrease of integration time with increasing light levels (as observed, Juusola and Hardie 2001). The feedback loop is assumed to operate as follows. An increase in [DAG], as occurs when the light level is increased, opens more TRP channels. This increases the photocurrent entering the cell. A considerable part of this photocurrent consists of Ca^{2+} ions, resulting in a rising Ca^{2+} concentration. This will then progressively increase the removal (or inactivation) rate of DAG (α). Therefore, the initial increase in [DAG] is counteracted by an increased removal of DAG, and the loop is thus a negative feedback loop. Because α in Eq. 7 depends on $[Ca^{2+}]$, an increase in $[Ca^{2+}]$ reduces both the gain, $1/\alpha$, and the time constant, τ_α, of DAG production. Although there is no direct evidence for a Ca^{2+}-dependent acceleration of DAG removal, DAG removal is part of a cycle eventually producing PIP_2. It is therefore possible that Ca^{2+} targetting other parts of this cycle (which is known to occur) might have a similar effect on the dynamics. An alternative to the above scheme, which can also produce $\beta^{0.5}$, is a direct Ca^{2+} feedback onto the TRP channels (Gu et al. 2005); in addition this requires an as yet unidentified time constant, the equivalent of τ_α, to depend on Ca^{2+} as well.

The relationship $I_p \sim \beta^{0.5}$, inferred from the experimental data of Oberwinkler and Stavenga (1998), is used in Fig. 4b to describe the transformation of steady-state β into steady-state photocurrent. The resulting compression is a first step towards equalizing the response to identical contrasts at different light intensities (Fig. 4a, b), and it also compresses the dynamic range of the responses to natural intensities (Fig. 4d–f).

The final processing stage, from photocurrent to membrane potential, is particularly nonlinear in blowfly photoreceptor cells, and has been well studied (Weckström et al. 1991; Juusola and Weckström 1993; Weckström and Laughlin 1995). Apart from self-shunting, several types of voltage-sensitive K^+ channels exist that make the current–voltage relationship strongly compressive. We will here represent this relationship only in a stylized way, where the curve in Fig. 4c assumes that the membrane potential V_p depends on the photocurrent I_p as $I_p^{0.25}$. As a result, the response to equal contrasts at different light intensities is fairly similar (Fig. 4c), and the pdf of the response is such that it fits well into the limited voltage response range of the cell (Fig. 4g).

Responses to natural stimuli

A clear signature of the performance of a photoreceptor is obtained by exposing it to natural stimuli with considerable temporal dynamics and encompassing a wide range of light intensities. Such stimuli were obtained by walking outdoors with a light detector (with an aperture of approximately 2 arcmin), whilst recording the intensities on a portable DAT-recorder (van Hateren 1997; van Hateren and Snippe 2001). Two minutes of such a time series (ts001, available from http://hlab.phys.rug.nl/archive.html) is shown in Fig. 5a, e (for the purpose of presentation filtered with a first-order low-pass filter with $\tau = 100$ ms; traces in Fig. 5b–d were similarly filtered). The 5-s surrounding $t = 60$ s in Fig. 5 is shown in Fig. 6a, e (for the purpose of presentation filtered with a first-order low-pass filter with $\tau = 3$ ms; traces in Fig. 6b–d were not filtered).

Primate cones are small and fragile, and it is therefore notoriously difficult to obtain long, stable recordings from these cells. We will therefore rely on simulations using a recently developed model of the cone (van Hateren 2005). This model incorporates established mechanisms of the phototransduction chain, and was developed as part of a larger model adequately describing recent measurements (Smith et al. 2001; Lee et al. 2003) in macaque horizontal cells (from which stable recordings are possible). For the blowfly the situation is reversed. Whereas the mechanisms of the phototransduction chain are insufficiently well known to make a complete, working, and physiologically realistic model, it is possible to record stably for extended periods of time from these cells. We will therefore rely on such measurements, which have been discussed before (van Hateren 1997; van Hateren and Snippe 2001). Below we will only compare the responses of the two photoreceptor types qualitatively; a detailed quantitative comparison is beyond the scope of this study.

Figures 5b and 6b show simulations of the response of a primate cone, and Figs. 5d and 6d show the response to the same stimulus as measured in a blowfly photoreceptor cell. By comparing Fig. 6b with d it is

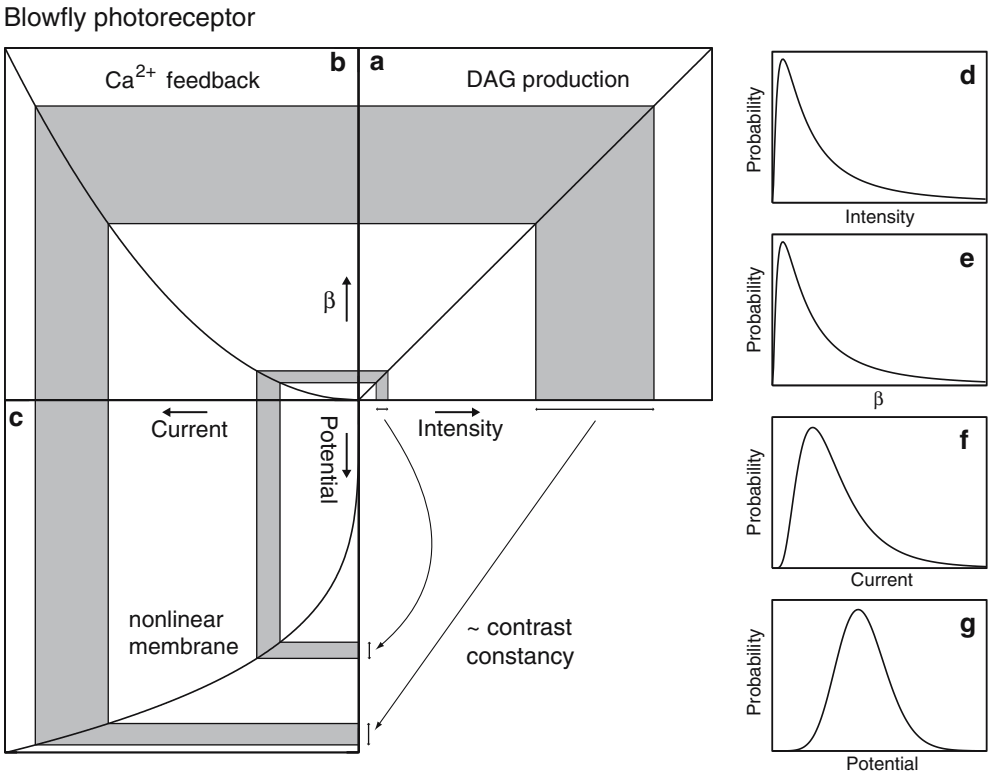

Fig. 4 Contrast constancy and range compression in blowfly photoreceptor cells. Identical contrasts at different light intensities I (*gray sections* at the intensity axis of **a**) transform linearly as $\beta \sim I$ due to DAG production by activated PLC. The calcium feedback loop transforms β approximately as $\beta^{0.5}$ into photocurrent (**b**). The nonlinear membrane of the cell is finally assumed to transform the photocurrent I_p as $I_p^{0.25}$ into the membrane potential of the cell (**c**). **d**–**g** The probability density of natural intensities (**d**, see Appendix) is gradually transformed by the nonlinearities of (**b**) and (**c**)

clear that not only the sign of the response is different, but also the integration time. It is indeed well known that blowfly photoreceptors are several times faster than primate cones (e.g., Juusola et al. 1994; Anderson and Laughlin 2000). To facilitate comparing the responses of these two photoreceptor types, a modified cone response was computed by reducing all time constants in the cone model by a factor of three, and inverting and shifting the resulting response (Figs. 5c, 6c). Comparing Figs. 5c with d and 6c with d shows that the responses of both types of photoreceptor cells are quite similar. In fact, to a first-order approximation they both follow the intensity when plotted on a logarithmic scale (Figs. 5e, 6e). The main difference between a simple logarithmic transformation and the responses of both types of photoreceptor is in the control of temporal bandwidth of the response. Whereas both photoreceptor types have a dynamic control of the integration time (through τ_β and τ_α), such a control is absent in the logarithmic transformation, which has a fixed, arbitrary integration time in Figs. 5e and 6e.

The histograms to the right of the traces in Fig. 5 show the distributions of the intensity and response values in the traces shown (cf. the theoretical probability density functions in Figs. 2, 4). It should be realized that the 2 min of data used for these histograms only represent a small and potentially biased sample of natural scenes, but the main change in statistics can be seen: the distribution of the intensity values (Fig. 5a) is quite skewed, while the distributions of the logarithm and the two types of photoreceptors are much more even.

Discussion

The mechanisms of phototransduction in primate cones and blowfly photoreceptors are quite different. They are not only using different molecules (e.g., PDE rather than PLC), but also different substrates for similar transformations (e.g., generating a strong nonlinearity by using a Ca^{2+} feedback, as in the cone, rather than by using voltage-sensitive channels in the membrane, as in the blowfly photoreceptor cell). But not only the physiological mechanisms are different, also the algorithms are. The cone approaches its goal boldly by immediately using a strong nonlinearity, $1/\beta$ due to cGMP hydrolysis, which overshoots its goal and is therefore subsequently counteracted by a strong Ca^{2+} feedback followed by a weaker membrane nonlinearity. The blowfly photoreceptor, on the other hand, approaches its goal more gradually from one direction only, using a moderately strong Ca^{2+} feedback followed by a strong membrane nonlinearity. Nevertheless, the overall result of both algorithms is quite similar (Figs. 5, 6).

The role of Ca^{2+} feedback is quite the opposite in the two types of photoreceptors. Whereas this feedback functions as a range expansion in the cone (partly reversing the effect of the $1/\beta$-nonlinearity), it functions as a range compression in the blowfly photoreceptor. Both cells are successful in obtaining range compression (Figs. 2g, 4g), such that the wide range of natural intensities (i.e., as encountered in a particular scene at a particular time of day) can be well coded in the cells'

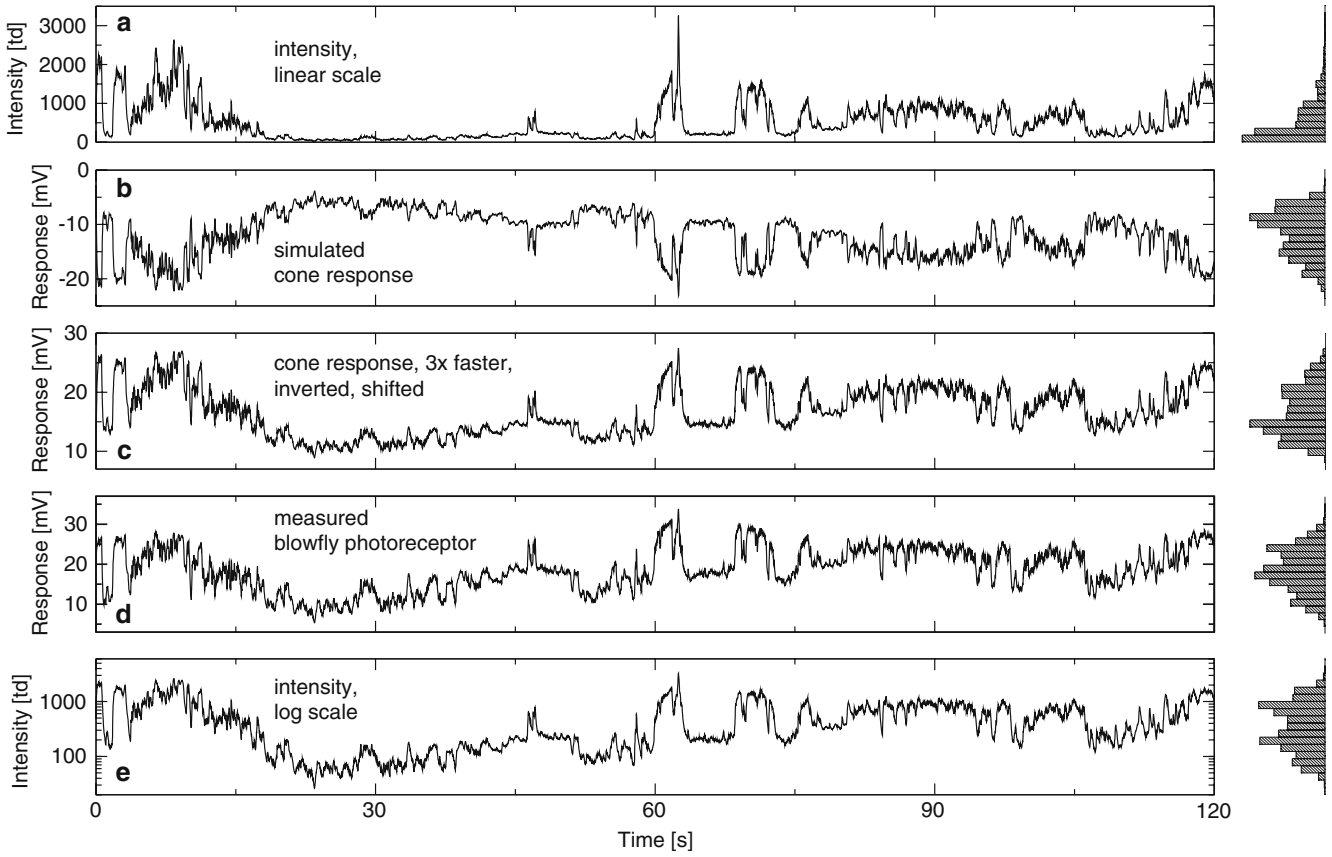

Fig. 5 Response of primate cone and blowfly photoreceptor to a natural time series of intensities. **a** Two minutes of a natural time series of intensities as measured outdoors. **b** Simulated response of a primate cone, using the cone model with generic parameter values as defined in van Hateren (2005). The response is shown relative to the membrane potential in the dark. **c** Same as (**b**) with all time constants in the model three times smaller than in (**b**); the resulting response was inverted, and shifted by 5 mV to facilitate comparison with (**d**). **d** Membrane potential, in response to the stimulus of (**a**), measured in a blowfly photoreceptor cell. **e** Same as (**a**), on a logarithmic scale. For the purpose of presentation, all traces at **a**–**e** are low-pass filtered using a first-order filter with a time constant $\tau = 100$ ms. The *histogram to the right* of each trace shows its probability density function

response ranges (see also Laughlin 1981, 1994). Similarly, both cells reach a state much closer to contrast constancy than the original stimulus (Figs. 2c, 4c). Finally, both cells control their integration time dynamically, although in quite different ways.

The similarity of the responses of cones and blowfly photoreceptors as discussed in this article is limited to bright, daylight conditions. When the light level is reduced, their performance strongly diverges. Whereas the function of cones is gradually taken over by the rods at low light levels, blowfly photoreceptors continue to function at such intensities, presumably by engaging additional mechanisms not included in Fig. 3. This continues up to the point where they give large (~1–2 mV) and fast (~30 ms integration time) responses to single photons.

Van Hateren and Snippe (2001) developed a phenomenological model for the blowfly photoreceptor cell, which adequately describes the responses to natural time series of intensities at high light levels. The model consists of two divisive gain control loops followed by a static nonlinearity. The first gain control loop produces a square-root steady-state nonlinearity, similar to that of the calcium feedback loop discussed here (Figs. 3, 4). The second divisive gain control loop contains a strongly expansive nonlinearity in the feedback path, and together with the final static nonlinearity this may have a similar function as the strong membrane nonlinearity discussed here (Fig. 4).

Hyperpolarizing and depolarizing photoreceptor cells

The most conspicuous difference between vertebrate and invertebrate photoreceptors is that, as a rule, the former are hyperpolarizing and the latter are depolarizing in response to increments of light intensity. This could have had a trivial cause, because the sign of the response depends on whether the transduction channels are opened or closed by the second messengers, and also on whether the photocurrent is flowing into or out of the cell. For primate cones and blowfly photoreceptors, however, both the action of cGMP (DAG) on the CNG (TRP) channels and the direction of the currents gated by these channels have the same sign. The fact that cones are hyperpolarizing and blowfly photoreceptors are de-

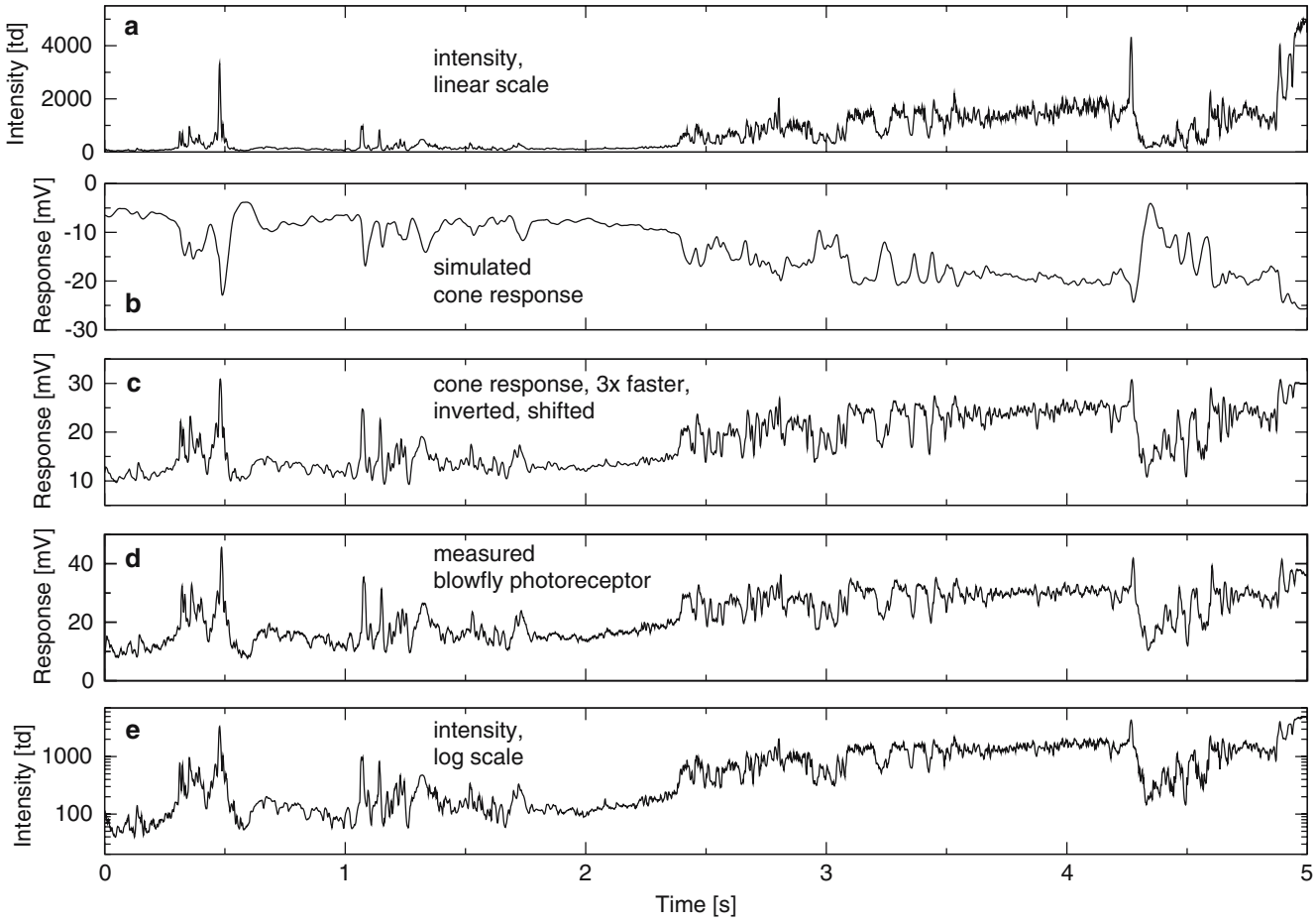

Fig. 6 Same as Fig. 5, for the segment 57.5–62.5 s of Fig. 5. The traces at (**a**) and (**e**) were filtered, for the purpose of presentation, with a low-pass filter with a time constant $\tau = 3$ ms; the traces at (**b**–**d**) were not filtered

polarizing therefore reflects the fundamentally different algorithms these cells, in essence, use: a sign-inverting $1/\beta$ nonlinearity due to cGMP hydrolysis in the case of cones (followed by an expansive Ca^{2+} feedback loop), versus a sign-conserving compressive cell membrane in the case of blowfly photoreceptors (following a compressive Ca^{2+} feedback loop). Nevertheless, the difference appears to be trivial from a functional point of view, because the response characteristics of the cells are quite similar (Figs. 5, 6).

Contrast constancy and the logarithmic transformation

As has been argued before for static responses (Normann and Werblin 1974; Laughlin and Hardie 1978; Normann and Perlman 1979; Laughlin 1981), photoreceptors are performing an operation resembling a logarithm. Taking a logarithm is, under static, noise-free conditions, clearly the short road to contrast constancy. This is because the response change to a contrast step c at a mean intensity I_0 is given by $\log((1+c)I_0) - \log I_0 = \log(1+c)$, and this response change is therefore independent of I_0. It is interesting to compare the details of the nonlinearities implemented in the two types of photoreceptors with a logarithm. Whereas the cone appears to produce a nonlinearity according to $1/\beta^{\mu}$, with μ small ($\mu \approx 0.12$, see van Hateren 2005), the blowfly photoreceptor appears to produce a nonlinearity according to β^{η}, with η small ($\eta = 0.5 \times 0.25 = 0.125$ in the stylized example as shown in Fig. 4). We can understand why these transformations resemble a logarithm by the fact that a logarithm can be written as either one of the following limits (e.g., The Wolfram functions site 2004)

$$\log \beta = \lim_{\varepsilon \to 0} \frac{1}{\varepsilon}(\beta^{\varepsilon} - 1) \tag{8}$$

$$-\log \beta = \lim_{\varepsilon \to 0} \frac{1}{\varepsilon}\left(\frac{1}{\beta^{\varepsilon}} - 1\right) \tag{9}$$

Apart from shifting (− 1) and scaling (1/ε), both β^{η} and $1/\beta^{\mu}$ can therefore be interpreted as attempts to reach something close to a logarithm.

The similarity of the response of cones and blowfly photoreceptors (Figs. 5, 6) to the result of a logarithmic transformation should not be overstated by saying that photoreceptors are just implementing a logarithm:

photoreceptors are not just acting as static non-linearities, but also perform dynamic operations. First of all, they low-pass filter the incoming intensities. More importantly, the amount of low-pass filtering (i.e., the integration time) depends on the light level. This dependence is an important mechanism to maximize the information transfer through the early parts of the visual system (blowfly: van Hateren 1992). Also in the macaque cone, the adaptive control of the integration time is performed quickly and continuously (van Hateren 2005). The variable integration time in both types of photoreceptors is effectively controlling the intensity-dependent level of noise in the stimulus due to the random arrival of photons. A logarithmic transformation without adaptive control of integration time would be defenseless against such changes in noise level.

Acknowledgements We like to thank Doekele Stavenga for useful comments on the manuscript. This research is supported by the Netherlands Organization for Scientific Research (NWO/ALW).

Appendix

Probability density of light intensities in natural environments

The logarithm of light intensities in natural environments (at a particular time of day) follows approximately a Gaussian probability density function (see Richards 1982, for theoretical arguments, see van der Schaaf 1998, p 58, for experimental evidence). Therefore

$$p(\log I) = \frac{1}{\sqrt{2\pi}\sigma}\exp\{-(\log I)^2/(2\sigma^2)\}, \qquad (10)$$

with I the intensity scaled such that $p(\log I)$ has zero mean, the logarithms have base e, and $\sigma = 1.11$ (equivalent to $\sigma = 0.48$ reported by van der Schaaf (1998) for logarithms with base 10). Transforming the pdf for $\log I$ to the corresponding pdf for I implies multiplying by $\mathrm{d}(\log I)\mathrm{d}I = 1/I$, producing the log-normal pdf

$$p(I) = \frac{1}{\sqrt{2\pi}\sigma}\frac{1}{I}\exp\{-(\log I)^2/(2\sigma^2)\}. \qquad (11)$$

Eq. 11 has been plotted in Figs. 2d and 4d.

References

Anderson JC, Laughlin SB (2000) Photoreceptor performance and the co-ordination of achromatic and chromatic inputs in the fly visual system. Vision Res 40:13–31

Burns ME, Baylor DA (2001) Activation, deactivation, and adaptation in vertebrate photoreceptor cells. Ann Rev Neurosci 24:779–805

Demontis GC, Cervetto L (2002) Vision: how to catch fast signals with slow detectors. News Physiol Sci 17:110–114

Fain GL, Matthews HR, Cornwall MC, Koutalos Y (2001) Adaptation in vertebrate photoreceptors. Physiol Rev 81:117–151

Gu Y, Oberwinkler J, Postma M, Hardie RC (2005) Mechanisms of light adaptation in *Drosophila* photoreceptors. Curr Biol 15:1228–1234

Hardie RC (2003) Regulation of TRP channels via lipid second messengers. Annu Rev Physiol 65:735–759

Hardie RC, Raghu P (2001) Phototransduction in *Drosophila melanogaster*. Nature 413:186–193

van Hateren JH (1992) Theoretical predictions of spatiotemporal receptive fields of fly LMCs, and experimental validation. J Comp Physiol A 171:157–170

van Hateren JH (1997) Processing of natural time series of intensities by the visual system of the blowfly. Vision Res 37:3407–3416

van Hateren JH (2005) A cellular and molecular model of response kinetics and adaptation in primate cones and horizontal cells. J Vision 5:331–347, http://journalofvision.org/5/4/5/, DOI 10.1167/5.4.5

van Hateren JH, Snippe HP (2001) Information theoretical evaluation of parametric models of gain control in blowfly photoreceptor cells. Vision Res 41:1851–1865

Hendersen SR, Reuss H, Hardie RC (2000) Single photon responses in *Drosophila* photoreceptors and their regulation by Ca^{2+}. J Physiol 524:179–194

Juusola M, Hardie RC (2001) Light adaptation in *Drosophila* photoreceptors: I. Response dynamics and signaling efficiency at 25°C. J Gen Physiol 117:3–25

Juusola M, Weckström M (1993) Band-pass filtering by voltage-dependent membrane in an insect photoreceptor. Neurosci Lett 154:84–88

Juusola M, Kouvalainen E, Järvilehto M, Weckström M (1994) Contrast gain, signal-to-noise ratio, and linearity in light-adapted blowfly photoreceptors. J Gen Physiol 104:593–621

Laughlin SB (1981) Neural principles in the peripheral visual systems of invertebrates. In: Autrum H (ed) Handbook of sensory physiology, vol VII/6B. Springer, Berlin Heidelberg New York, pp 133–280

Laughlin SB (1994) Matching coding, circuits, cells, and molecules to signals—general principles of retinal design in the fly's eye. Progr Ret Eye Res 13:165–196

Laughlin SB, Hardie RC (1978) Common strategies for light adaptation in the peripheral visual systems of fly and dragonfly. J Comp Physiol 128:319–340

Lee BB, Dacey DM, Smith VC, Pokorny J (2003) Dynamics of sensitivity regulation in primate outer retina: the horizontal cell network. J Vision 3:513–526, http://journalofvision.org/3/7/5/, DOI 10.1167/3.7.5

Minke B, Hardie RC (2000) Genetic dissection of *Drosophila* phototransduction. In: Stavenga DG, de Grip WJ, Pugh EN Jr (eds) Handbook of biological physics, vol 3. Elsevier, Amsterdam, pp 449–525

Montell C (1999) Visual transduction in *Drosophila*. Annu Rev Cell Dev Biol 15:231–268

Nasi E, Del Pilar Gomez M, Payne R (2000) Phototransduction mechanisms in microvillar and ciliary photoreceptors in invertebrates. In: Stavenga DG, de Grip WJ, Pugh EN Jr (eds) Handbook of biological physics, vol 3. Elsevier, Amsterdam, pp 389–448

Nikonov S, Lamb TD, Pugh EN Jr (2000) The role of steady phosphodiesterase activity in the kinetics and sensitivity of the light-adapted salamander rod photoresponse. J Gen Physiol 116:795–824

Normann RA, Perlman I (1979) Evaluating sensitivity changing mechanisms in light-adapted photoreceptors. Vision Res 19:391–394

Normann RA, Werblin FS (1974) Control of retinal sensitivity. I. Light and dark adaptation of vertebrate rods and cones. J Gen Physiol 63:37–61

Oberwinkler J, Stavenga DG (1998) Light dependence of calcium and membrane potential measured in blowfly photoreceptors in vivo. J Gen Physiol 112:113–124

Pugh EN Jr, Lamb TD (2000) Phototransduction in vertebrate rods and cones: Molecular mechanisms of amplification, recovery and light adaptation. In: Stavenga DG, de Grip WJ, Pugh EN Jr (eds) Handbook of biological physics, vol 3. Elsevier, Amsterdam, pp 183–254

Richards WA (1982) Lightness scale from image intensity distributions. Appl Optics 21:2569–2582

van der Schaaf A (1998) Natural image statistics and visual processing. PhD thesis, University of Groningen, http://irs.ub.rug.nl/ppn/166956252

Smith VC, Pokorny J, Lee BB, Dacey DM (2001) Primate horizontal cell dynamics: an analysis of sensitivity regulation in the outer retina. J Neurophysiol 85:545–558

The Wolfram functions site (2004) http://functions.wolfram.com/01.04.09.0001.01

Weckström M, Laughlin SB (1995) Visual ecology and voltage-gated ion channels in insect photoreceptors. Trends Neurosci 18:17–21

Weckström M, Hardie RC, Laughlin SB (1991) Voltage-activated potassium channels in blowfly photoreceptors and their role in light adaptation. J Physiol 440:635–657